Estimating Equivalent Dipole Polarizabilities for the Inductive Response of Isolated Conductive Bodies

J Torquil Smith, H Frank Morrison
Lawrence Berkeley National Laboratory
Berkeley, California 94720

ABSTRACT

Away from a conductive body, secondary magnetic fields due to currents induced in the body by a time varying external magnetic field are approximated by (equivalent) magnetic dipole fields. Approximating the external magnetic field by its value at the location of the equivalent magnetic dipoles, the equivalent magnetic dipoles' strengths are linearly proportional to the external magnetic field, for a given time dependence of external magnetic field, and are given by the equivalent dipole polarizability matrix. The polarizability matrix and its associated equivalent dipole location is estimated from magnetic field measurements made with at least three linearly independent polarizations of external magnetic fields at the body.

Uncertainties in the polarizability matrix elements and its equivalent dipole location are obtained from analysis of a linearized inversion for polarizability and dipole location. Polarizability matrix uncertainties are independent of the scale of the polarizability matrix. Dipole location uncertainties scale inversely with the scale of the polarizability matrix. Uncertainties in principal polarizabilities and directions are obtained from the sensitivities of eigenvectors and eigenvalues to perturbations of a symmetric matrix. In application to synthetic data from a magnetic conducting sphere and to synthetic data from an axially symmetric elliptic conducting body, the estimated polarizability matrices, equivalent dipole locations and principal polarizabilities and directions are consistent with their estimated uncertainties.

INTRODUCTION

Equivalent dipoles have long been used for approximating potential fields in geophysics as well other fields, and we will not attempt to outline the history of their usage. Recently, they have been used to model secondary magnetic fields arising from currents induced in isolated conductive, and possibly magnetic bodies, for discrimination between unexploded ordnance (UXO) and other materials, for example, by Khadr *et al*. (1998), Bell *et al*. (2001), Pasion and Oldenburg (2001), or Baum (1999). In these recent examples, the induced dipoles are modelled as linearly proportional to the inducing magnetic fields at the body centers. Since the inducing magnetic fields are, in general, vector, and the induced dipoles may have components in x, y and z directions, the two are related by a matrix. Baum develops equivalent dipole polarization matrices starting from a treatment of properties of low frequency scatterers. Here, we develop them keeping assumptions to a minimum.

Any set of currents can be characterized in terms of a set of multipole moments of the currents. The associated magnetic fields can be represented as a sum of corresponding multipole terms away from the currents (e.g., Jackson, 1975, p.746). For a magnetic multipole term of order n, magnetic field strengths fall off as $1/r^{n+2}$, in resistive media. Dipole terms are the lowest order magnetic multipole terms. At distances much greater than the scale of an object, dipole terms become a very good approximation to the magnetic fields arising from currents induced in the object.

In the vicinity of a conductive body, the primary magnetic field imposed by an external source current may be approximated by the primary magnetic field at the objects center $\mathbf{r}_o$, $\mathbf{B}^{(p)}(\mathbf{r}_o,t)$. Assuming a common time variation $g(t)$ for all primary magnetic field components at the object center, we define a primary field magnitude vector as $\mathbf{B}^{(o)} \equiv \mathbf{B}^{(p)}(\mathbf{r}_o,t)/g(t)$. We choose the normalization of $g(t)$ so that $g(t_o)$=1 at some chosen time t_o, for example, for a step function turn-off primary field we choose the scale of $g(t)$ so that $g(t)$=1 for t<0. In practice, it is common to assume that the medium surrounding the object is sufficiently resistive that magnetic fields due to currents induced in the surrounding medium are negligible at the body, so that $g(t)$

is simply the transmitter current waveform. Neglecting primary field gradients, the secondary magnetic fields

$$\mathbf{B}^{(s)}(\mathbf{r},t) \equiv \mathbf{B}(\mathbf{r},t) - \mathbf{B}^{(p)}(\mathbf{r},t) \tag{1}$$

due to currents induced in a conductive body can be written as linear combinations of the magnetic fields that would be induced by primary fields of strength $g(t)$ in the $\hat{\mathbf{x}}$, $\hat{\mathbf{y}}$, or $\hat{\mathbf{z}}$ direction at the objects center, $\mathbf{B}_x^{(s)}(\mathbf{r},t)$, $\mathbf{B}_y^{(s)}(\mathbf{r},t)$, or $\mathbf{B}_z^{(s)}(\mathbf{r},t)$ respectively;

$$\mathbf{B}^{(s)}(\mathbf{r},t) = B_x^{(o)}\,\mathbf{B}_x^{(s)}(\mathbf{r},t) + B_y^{(o)}\,\mathbf{B}_y^{(s)}(\mathbf{r},t) + B_z^{(o)}\,\mathbf{B}_z^{(s)}(\mathbf{r},t) \quad , \tag{2}$$

where $B_x^{(o)}$, $B_y^{(o)}$, and $B_z^{(o)}$ are the x, y, and z components of $\mathbf{B}^{(o)}$, that is,

$$\mathbf{B}^{(s)}(\mathbf{r},t) = \left[\mathbf{B}_x^{(s)}(\mathbf{r},t),\ \mathbf{B}_y^{(s)}(\mathbf{r},t),\ \mathbf{B}_z^{(s)}(\mathbf{r},t)\right] \cdot \mathbf{B}^{(o)} \quad , \tag{3}$$

where, with $\mathbf{B}^{(s)}(\mathbf{r},t)$, $\mathbf{B}_x^{(s)}(\mathbf{r},t)$, $\mathbf{B}_y^{(s)}(\mathbf{r},t)$, $\mathbf{B}_z^{(s)}(\mathbf{r},t)$, and $\mathbf{B}^{(o)}$ considered as column vectors, the dot effects matrix multiplication.

At distances where non-dipole secondary magnetic fields are small, the secondary magnetic fields induced by the primary magnetic field in the $\hat{\mathbf{x}}$ direction can be broken into contributions by dipole components in the x, y, and z directions;

$$\mathbf{B}_x^{(s)}(\mathbf{r},t) = m_{xx}(t)\,\mathbf{B}_x^{(d)}(\mathbf{r}) + m_{yx}(t)\,\mathbf{B}_y^{(d)}(\mathbf{r}) + m_{zx}(t)\,\mathbf{B}_z^{(d)}(\mathbf{r}) \quad , \tag{4a}$$

where $\mathbf{B}_x^{(d)}(\mathbf{r})$, $\mathbf{B}_y^{(d)}(\mathbf{r})$, and $\mathbf{B}_z^{(d)}(\mathbf{r})$ are the magnetic fields of a unit magnetic dipole in the $\hat{\mathbf{x}}$, $\hat{\mathbf{y}}$, and $\hat{\mathbf{z}}$ directions respectively, placed at the body center, $m_{xx}(t)$, $m_{yx}(t)$, and $m_{zx}(t)$ are the effective magnetic dipole moments in these directions, for a unit primary (inducing) magnetic field in the $\hat{x}$ direction at the object center. Similarly,

$$\mathbf{B}_y^{(s)}(\mathbf{r},t) = m_{xy}(t)\,\mathbf{B}_x^{(d)}(\mathbf{r}) + m_{yy}(t)\,\mathbf{B}_y^{(d)}(\mathbf{r}) + m_{zy}(t)\,\mathbf{B}_z^{(d)}(\mathbf{r}) \quad , \tag{4b}$$

$$\mathbf{B}_z^{(s)}(\mathbf{r},t) = m_{xz}(t)\,\mathbf{B}_x^{(d)}(\mathbf{r}) + m_{yz}(t)\,\mathbf{B}_y^{(d)}(\mathbf{r}) + m_{zz}(t)\,\mathbf{B}_z^{(d)}(\mathbf{r}) \quad , \tag{4c}$$

with $m_{xy}(t)$, $m_{yy}(t)$, $m_{zy}(t)$, and $m_{xz}(t)$, $m_{yz}(t)$, $m_{zz}(t)$ the corresponding moments for unit primary magnetic fields in the $\hat{\mathbf{y}}$ and $\hat{\mathbf{z}}$ directions. Assuming that the surrounding medium is sufficiently resistive that tertiary currents induced in the surrounding medium by the magnetic fields due to currents in the body can be neglected, the effective magnetic dipole moments correspond to the actual moments of the currents

circulating in the body. We make this assumption, and henceforth refer to them simply as the dipole moments. Equations (4) can be written in matrix form as

$$\left[\mathbf{B}_x^{(s)}(\mathbf{r}), \mathbf{B}_y^{(s)}(\mathbf{r}), \mathbf{B}_z^{(s)}(\mathbf{r}) \right] = \left[\mathbf{B}_x^{(d)}(\mathbf{r}), \mathbf{B}_y^{(d)}(\mathbf{r}), \mathbf{B}_z^{(d)}(\mathbf{r}) \right] \begin{bmatrix} m_{xx} & m_{xy} & m_{xz} \\ m_{yx} & m_{yy} & m_{yz} \\ m_{zx} & m_{zy} & m_{zz} \end{bmatrix} , \quad (5)$$

where the explicit time dependence of the matrix of dipole moments has been omitted. The matrix of dipole moments **M** is symmetric (Landau and Lifshitz, 1960, p192). Substituting equation (5) into equation (3) gives

$$\mathbf{B}^{(s)}(\mathbf{r},t) = \left[\mathbf{B}_x^{(d)}(\mathbf{r}), \mathbf{B}_y^{(d)}(\mathbf{r}), \mathbf{B}_z^{(d)}(\mathbf{r}) \right] \mathbf{M}(t) \ \mathbf{B}^{(o)} \quad . \quad (6)$$

In time domain applications, **M** is real, in addition to being symmetric, so can be diagonalized by an orthogonal matrix $\mathbf{U}(t)$;

$$\mathbf{L}(t) = \mathbf{U}^T(t) \ \mathbf{M}(t) \ \mathbf{U}(t) \quad , \quad (7)$$

where $\mathbf{L}(t)$ is diagonal, with elements $L_{11}(t)$, $L_{22}(t)$, $L_{33}(t)$ known as the principal moments (eigenvalues) of $\mathbf{M}(t)$, and ^{T} denotes transpose. Equation (7) expresses $\mathbf{M}(t)$ in coordinates given by the columns of $\mathbf{U}(t)$, ($\mathbf{u}_i$), known as the principal directions of $\mathbf{M}(t)$. For bodies with an axis of symmetry $\hat{\mathbf{w}}$, $\hat{\mathbf{w}}$ is a principal direction (e.g., $\mathbf{u}_1$), with corresponding principal component (e.g., L_{11}) giving the equivalent dipole moment induced in the $\hat{\mathbf{w}}$ direction for a unit primary field in the $\hat{\mathbf{w}}$ direction at the object center. The other two principal moments correspond to equivalent dipole moments induced in directions normal to $\hat{\mathbf{w}}$ for unit primary fields in those directions. Symmetry of the object implies that the latter two moments are equal. For a symmetric object, rotating into coordinates aligned with the object's symmetry axis diagonalizes **M**, so may be accomplished by a rotation matrix **U**, which is independent of time.

This definition of the equivalent dipole polarizability matrix **M** is consistent with that used by Pasion and Oldenburg (2001), and differs by a factor of μ_o from that used by Baum (1999).

As written, equation (6) represents the magnetic field $\mathbf{B}^{(s)}(\mathbf{r},t)$ as a linear combination of dipole fields. Differentiating it, one can apply the same methods to modelling measurements of $d\mathbf{B}^{(s)}(\mathbf{r},t)/dt$, with $d\mathbf{M}(t)/dt$ replacing $\mathbf{M}(t)$.

For a given time dependence of source, $g(t)$, equation (6) relates secondary fields at any time to an equivalent dipole polarizability $\mathbf{M}(t)$ for that time, so $\mathbf{M}(t)$ may be estimated separately for each time. Consequently, we drop the explicit time dependence, and assume that all measurements are at a single time relative to the starting time for the primary field pulse.

ESTIMATING DIPOLE POLARIZABILITIES WHEN OBJECT CENTER IS KNOWN

When the object center location is known, $\mathbf{B}^{(o)}$ can be calculated for each of a set of sources with the same time dependence $g(t)$. For the i'th measurement of a set of n measurements, letting $\mathbf{B}_i^{(o)}$ be the primary field polarization vector at the object center for the source used for that measurement, $\mathbf{r}_i$ be the location of a magnetic field measurement, and $\hat{\mathbf{v}}_i$ be the orientation of the magnetic field receiver (e.g., coil), equation (6) written for the $\hat{\mathbf{v}}_i$ component at $\mathbf{r}_i$ is

$$\hat{\mathbf{v}}_i^T\,\mathbf{B}^{(s)}(\mathbf{r}_i) = \hat{\mathbf{v}}_i^T\cdot\left[\mathbf{B}_x^{(d)}(\mathbf{r}_i),\mathbf{B}_y^{(d)}(\mathbf{r}_i),\mathbf{B}_z^{(d)}(\mathbf{r}_i)\right]\;\mathbf{M}\;\mathbf{B}_i^{(o)}\quad, \tag{8}$$

one (scalar) equation constraining the six unknown dipole polarizabilities m_{xx}, m_{yy}, m_{zz}, $m_{xy}=m_{yx}$, $m_{yz}=m_{zy}$, and $m_{xz}=m_{zx}$, for each receiver source combination. This can be rewritten as

$$d_i = f_{i\,xx}\,m_{xx} + f_{i\,yy}\,m_{yy} + f_{i\,zz}\,m_{zz} + f_{i\,xy}\,m_{xy} + f_{i\,yz}\,m_{yz} + f_{i\,xz}\,m_{xz}\quad, \tag{9}$$

where $d_i \equiv \hat{\mathbf{v}}_i^T\,\mathbf{B}^{(s)}(\mathbf{r}_i)$, and the coefficients $f_{i\,xx}$, $f_{i\,yy}$, $\cdots$, can be found by multiplying out the vector and matrix products on the right side of equation (8), substituting m_{xy}, m_{yz}, and m_{xz} for m_{yx}, m_{zy}, and m_{zx}, and identifying the coefficients of m_{xx}, m_{yy}, m_{zz}, m_{xy}, m_{yz}, and m_{xz}. Equations (9) can be written in matrix form as

$$\mathbf{d} = \mathbf{F}\,\mathbf{m}\quad, \tag{10}$$

where $\mathbf{m} \equiv (m_{xx},m_{yy},m_{zz},m_{xy},m_{yz},m_{xz})^T$. For data with correlated measurement errors

with correlation matrix $\mathbf{C}_d$, we use estimate

$$\mathbf{m} = (\mathbf{F}^T\, \mathbf{C}_d^{-1}\, \mathbf{F})^{-1}\, \mathbf{F}^T\, \mathbf{C}_d^{-1}\, \mathbf{d} \quad . \tag{11}$$

For data with uncorrelated errors, $\mathbf{C}_d^{-1}$ is diagonal, with the inverse squared measurement errors $1/\sigma^2$ on its diagonal: the $\mathbf{C}_d^{-1}$ terms in equation (11) effectively weight the rows of equations (10) by $1/\sigma$. In the case of equal independent measurement errors, this reduces to least squares solution

$$\mathbf{m} = (\mathbf{F}^T\, \mathbf{F})^{-1}\, \mathbf{F}^T\, \mathbf{d} \quad .$$

The dipole polarizability moment matrix $\mathbf{M}$ can be assembled from the elements of $\mathbf{m}$, using the symmetry of $\mathbf{M}$.

ESTIMATING DIPOLE POLARIZABILITIES AND OBJECT CENTER LOCATION

When the object center position $\mathbf{r}_o$ is unknown, one may form equation (8) using dipole fields $\mathbf{B}_x^{(d)}$, $\mathbf{B}_y^{(d)}$, $\mathbf{B}_z^{(d)}$ calculated for dipoles centered at some candidate object center position $\mathbf{r}_o$, and primary field polarization vectors $\mathbf{B}_i^{(o)}$ at the candidate object center position, form equation (10), and calculate the least squares dipole polarizabilities $\mathbf{m}$ for that candidate center location, $\mathbf{m}(\mathbf{r}_o)$. Its squared weighted misfit is

$$\chi^2 \equiv [\, \mathbf{d} - \hat{\mathbf{d}}(\mathbf{r}_o)\,]^T\ \mathbf{C}_d^{-1}\ [\, \mathbf{d} - \hat{\mathbf{d}}(\mathbf{r}_o)\,] \tag{12}$$

where

$$\hat{\mathbf{d}}(\mathbf{r}_o) \equiv \mathbf{F}\ (\mathbf{F}^T\, \mathbf{C}_d^{-1}\, \mathbf{F})^{-1}\ \mathbf{F}^T\, \mathbf{C}_d^{-1}\, \mathbf{d} \tag{13}$$

is the best fitting data predicted for this choice of $\mathbf{r}_o$. Matrix $\mathbf{F}$ depends on $\mathbf{r}_o$ through $\mathbf{B}_x^{(d)}$, $\mathbf{B}_y^{(d)}$, $\mathbf{B}_z^{(d)}$, and $\mathbf{B}_i^{(o)}$. We find the position $\mathbf{r}_o$ giving a minimum of squared misfit (12), using the downhill simplex algorithm (Press, *et al.*, 1986, p289), started from four candidate center locations, $\mathbf{r}_o^{(j)}$, j=1,...,4 at the corners of a tetrahedron with edges one quarter of the length of the maximum separation of receiver locations, centered one half the maximum receiver separation below the receivers. The downhill simplex algorithm moves the corners of the tetrahedron systematically expanding or contracting as necessary to arrive at a minimum of the minimized function, (the

squared misfit), and ends when the corners have converged within a small tolerance of each other, or the function values at the four corners are within a small tolerance of each other.

The downhill simplex method works well when there is only one mimimum in the area that it searchs, to which it converges. When there are more than one minimum in the searched area which minimum is arrived at is indeterminate. It has the advantage of being very rapid compared to more general methods of non-linear optimization which, in the limit of infinitely slow convergence, are able to avoid being stuck in merely local minima. For transmitter-receiver combinations for which local minima are known to exist close to the global minimum other non-linear optimization methods or a grid search may be appropriate to find the global minimum.

ESTIMATING DIPOLE POLARIZABILITY UNCERTAINTIES

For data with small measurement errors, the uncertainty in the resultant dipole polarizabilities and equivalent dipole position (object center) may be obtained from analysis of a linearized inversion for dipole polarizabilities and position. Denoting x, y, and z components of the center primary field $\mathbf{B}_i^{(o)}$ by $B_{1i}^{(o)}$, $B_{2i}^{(o)}$, and $B_{3i}^{(o)}$, and numbering the elements of $\mathbf{M}$ as m_{kj}, for k=1,3, j=1,3, then equation (8) can be written explicitly as

$$d_i = \sum_{k=1}^{3} \sum_{j=1}^{3} B'^{(d)}_{ik} \, B_{ji}^{(o)} \, m_{kj} \quad , \tag{14}$$

where,

$$B'^{(d)}_{i1} \equiv \hat{\mathbf{v}}_i^T \cdot \mathbf{B}_x^{(d)}(\mathbf{r}_i) \quad , \quad B'^{(d)}_{i2} \equiv \hat{\mathbf{v}}_i^T \cdot \mathbf{B}_y^{(d)}(\mathbf{r}_i) \quad , \quad B'^{(d)}_{i3} \equiv \hat{\mathbf{v}}_i^T \cdot \mathbf{B}_z^{(d)}(\mathbf{r}_i) \quad . \tag{15}$$

When equivalent dipole position $\mathbf{r}_o$ is not known *a priori*, one can expand equation (14) in a Taylor series about an initial value $\mathbf{r}_o^{(q)}$, such as the result of the downhill simplex method search of the previous section. Letting $\mathbf{M}^{(q)}$ be the corresponding dipole polarizability matrix fit for candidate dipole position $\mathbf{r}_o^{(q)}$, a first order Taylor expansion about $\mathbf{r}_o^{(q)}$ yields

$$d_i = \sum_{k=1}^{3} \sum_{j=1}^{3} \left\{ B'^{(d)}_{ik} B^{(o)}_{ji} m^{(q+1)}_{kj} + m^{(q)}_{kj} \left[\mathbf{r}_o^{(q+1)} - \mathbf{r}_o^{(q)} \right]^T \cdot \nabla_{\mathbf{r}_o} \left[B'^{(d)}_{ik} B^{(o)}_{ji} \right] \right\} . \quad (16)$$

Collecting coefficients of the new polarizability estimates $m_{11}^{(q+1)}$, $m_{22}^{(q+1)}$, ..., into a row vector $\mathbf{a}_i^{(q)}$, and coefficients of the components of change vector $\Delta\mathbf{r}_o \equiv \mathbf{r}_o^{(q+1)} - \mathbf{r}_o^{(q)}$ into a row vector $\mathbf{g}_i^{(q)}$ equation (16) becomes

$$d_i = \left[\mathbf{a}_i^{(q)}, \mathbf{g}_i^{(q)} \right] \left[m_{11}, m_{22}, m_{33}, m_{12}, m_{23}, m_{13}, \Delta x_o, \Delta y_o, \Delta z_o \right]^T , \quad (17)$$

where superscript $(q+1)$ has been omitted from the various $m_{ij}^{(q+1)}$, and the symmetry of $\mathbf{M}$ has been used to eliminate $m_{21}^{(q+1)}$, $m_{32}^{(q+1)}$, and $m_{31}^{(q+1)}$. This can be written in matrix form as

$$\mathbf{d} = \tilde{\mathbf{F}}\, \tilde{\mathbf{m}} , \quad (18)$$

where the rows of $\tilde{\mathbf{F}}$ and vector $\tilde{\mathbf{m}}$ are the vectors on the right side of equation (17), and solved for $\tilde{\mathbf{m}}$ in the same manner as equations (10) and (11). A new estimated object center position is given by

$$\mathbf{r}_o^{(q+1)} = \mathbf{r}_o^{(q)} + \Delta\mathbf{r}_o . \quad (19)$$

Taylor expanding about the new estimate $\mathbf{r}_o^{(q+1)}$ (equation 16, with q incremented), the process is repeated until the change magnitude $|\Delta\mathbf{r}_o|$ is less than a small tolerance. The variances of the resultant dipole polarizabilities m_{xx}, m_{yy}, m_{zz}, m_{xy}, m_{yz}, m_{xz}, and equivalent dipole coordinates x_o, y_o, and z_o, are given by the diagonal elements of the covariance matrix

$$cov(\tilde{\mathbf{m}}) = (\tilde{\mathbf{F}}^T \mathbf{C}_d^{-1} \tilde{\mathbf{F}})^{-1}. \quad (20)$$

For magnetic field measurements with squared uncertainty σ^2 and noise uncorrelated between receivers, $\mathbf{C}_d = diag(\sigma^2)$ is a diagonal matrix, and

$$cov(\tilde{\mathbf{m}}) = (\tilde{\mathbf{F}}^T \tilde{\mathbf{F}})^{-1} \sigma^2 . \quad (21)$$

A close examination of the structure of equations (16), (17), and (18) reveals some properties of the scaling of estimation uncertainties with the scale of the polarizability matrix, that are useful for comparing estimate uncertainty levels for a given set

of receivers and transmitters recording data from similar objects of varying size. In equation (17) the coefficients $\mathbf{a}_i^{(q)}$ of the updated polarizability matrix elements depend only on equivalent dipole position $\mathbf{r}_o^{(q)}$, not on the polarizability matrix; the coefficients $\mathbf{g}_i^{(q)}$ of the equivalent dipole position update $\Delta\mathbf{r}_o$, scale linearly with changes in scale of the current estimated polarizability matrix. That is, the coefficients in equations (17) and (18) written for data from an object with polarizability matrix $\mathbf{M}$, and from an object with polarizability matrix $\alpha\mathbf{M}$, differ only in that in the latter case coefficients $\mathbf{g}_i^{(o)}$ are scaled by a factor of α. In this case, the coefficient matrix in equations rewritten for unknown vector $(m_{11}, m_{22}, m_{33}, m_{12}, m_{23}, m_{13}, \alpha\Delta x_o, \alpha\Delta y_o, \alpha\Delta z_o)^T$ are identical in the two cases. This implies that the estimation uncertainties for the polarizabilty matrix elements are identical in the two cases. The relative uncertainties in polarizability matrix elements are, of course, proportionally smaller when the polarizability matrix elements are larger. The same consideration of scaling implies that the uncertainties in estimated equivalent dipole position vary inversely with the polarizability matrix scale α: if an object has a polarizabilities that are twice those of another object, the uncertainties in its estimated location are one half those of the former object at the same location and orientation relative to the system of transmitters and receivers. This argument is strictly valid in the limit of small location estimation errors, as it depends on the coefficicient matrix $\tilde{\mathbf{F}}$ being evaluated for equivalent dipoles at the same location in the two cases.

The uncertainty estimates presented here depend on the coefficient matrix $\tilde{\mathbf{F}}$ being evaluated with equivalent dipole position at the minimum squared misfit χ^2. If evaluated at a position far from the global minimum they may be inaccurate due to differences in the coefficient matrix from its value at the global minimum.

When evaluating uncertainty estimates from inversion of data with noise, the uncertainty estimates depend weakly on the specific values of the noise in the data, that is, on the realization of the noise. A different noise realization will yield different estimates of the equivalent dipole position and polarizability matrix: the coefficient matrix $\tilde{\mathbf{F}}$ will evaluate slightly differently, yielding different uncertainty estimates. For

comparing the performance of different transmitter-receiver configurations, one can eliminate the dependence of uncertainty estimates on the particular realisation of noise added to simulated data, by evaluating the coefficient matrix using the true object position and polarizability matrix, and using it in equation (20) or (21), to yield an estimated covariance matrix $\overline{cov}(\tilde{\mathbf{m}})$. The diagonal of this covariance matrix yields the expected values of the uncertainties, which obey the scaling relationships exactly.

PRINCIPAL MOMENT AND PRINCIPAL DIRECTION UNCERTAINTIES

The leading six by six sub-matrix of $cov(\tilde{\mathbf{m}})$ gives the covariance of the non-redundant elements of the dipole polarizability matrix $\mathbf{M}$, $cov(\mathbf{m})$. The principal directions of $\mathbf{M}$ are given by the eigenvectors of $\mathbf{M}$, and form the columns of the rotation matrix $\mathbf{U}$ which diagonalizes $\mathbf{M}$ (equation 7), yielding its the principal moments on the diagonal. Using the symmetry of $\mathbf{M}$ and $\mathbf{L}$, equation (7) can be written as

$$\mathbf{l}_L = \mathbf{O}\ \mathbf{m} \tag{22}$$

where $\mathbf{l}_L \equiv (L_{11}, L_{22}, L_{33}, L_{12}, L_{23}, L_{13})^T$, and $\mathbf{O}$ is an orthogonal matrix obtained by writing out matrix product (7) explicitly and identifying coefficients of the various m_{ij}, in the corresponding equation for each element $L_{i'j'}$. Principal moments L_{11}, L_{22}, L_{33} are Rayleigh quotients of matrix $\mathbf{M}$, so are insensitive, to first order, to changes in estimated principal direction matrix $\mathbf{U}$. Their squared uncertainties lie on the diagonal of

$$cov(\mathbf{l}_L) = \mathbf{O}\ cov(\mathbf{m})\ \mathbf{O}^T \quad . \tag{23}$$

Uncertainties in the principal directions of $\mathbf{M}$ are related to the stability of eigenvectors of $\mathbf{M}$ to changes in $\mathbf{M}$. Perturbing $\mathbf{M}$ by $\Delta\mathbf{M}$, the resulting change in the j'th eigenvector (principal direction) $\mathbf{u}_j$ is

$$\Delta\mathbf{u}_j = \sum_{k\neq j} \frac{\mathbf{u}_k^T\ \Delta\mathbf{M}\ \mathbf{u}_j}{\lambda_j - \lambda_k}\ \mathbf{u}_k \tag{24}$$

to first order in $\Delta\mathbf{M}$, provided that $\lambda_j \neq \lambda_k$ for $k \neq j$, where λ_k are eigenvalues of $\mathbf{M}$ (L_{11}, L_{22}, and L_{33}) (Watson, 1983). The numerator can be written as

$$\mathbf{u}_k^T\ \Delta\mathbf{M}\ \mathbf{u}_j = \mathbf{w}_{jk}^T\ \Delta\mathbf{m} \tag{25}$$

where $\mathbf{w}_{jk}^T \equiv (u_{1j}u_{1k},\ u_{2j}u_{2k},\ u_{3j}u_{3k},\ u_{1j}u_{2k}+u_{2j}u_{1k},\ u_{2j}u_{3k}+u_{3j}u_{2k},\ u_{1j}u_{3k}+u_{3j}u_{1k})$. The squared uncertainties of the elements of the j'th principal direction are then given by the diagonal elements of the three by three matrix

$$cov(\mathbf{u}_j) = \left[\sum_{k\neq j} \frac{\mathbf{u}_k\,\mathbf{w}_{jk}^T}{\lambda_j-\lambda_k}\right] cov(\mathbf{m}) \left[\sum_{k\neq j} \frac{\mathbf{u}_k\,\mathbf{w}_{jk}^T}{\lambda_j-\lambda_k}\right]^T \quad . \tag{26}$$

If some eigenvalue λ_k is very close to λ_j the denominator in equation (24) becomes small, and a perturbation $\Delta\mathbf{M}$ may perturb the j'th eigenvector a large amount in the direction of the k'th eigenvector. Consequently, the principal directions corresponding to two principal moments are poorly determined when the difference between the two moments is less than the uncertainty in their difference. The squared uncertainty in the difference between the i'th and j'th principal moments is

$$var(L_{ii}-L_{jj}) = cov(\mathbf{l}_L)_{ii} + cov(\mathbf{l}_L)_{jj} - 2\,cov(\mathbf{l}_L)_{ij} \quad , \tag{27}$$

where $cov(\mathbf{l}_L)_{ij}$ is the ij'th element of $cov(\mathbf{l}_L)$.

APPLICATION

Our current application of equivalent dipole polarizabilities is discrimination amongst buried metallic objects. The authors' encoding of the preceeding algorithms have been extensively tested on synthetic data. Two synthetic examples are presented here.

The first example simulates collection of magnetic induction data in the vicinity of a 12 cm diameter buried steel sphere with a relative permeability $\mu_r = 180$, and conductivity $\sigma = 10^7\ \Omega^{-1}\mathrm{m}^{-1}$, with the sphere center 1 m below the level of transmitter and receiver coils. Three components of the time derivative of the secondary magnetic induction $d\mathbf{B}^{(s)}/dt$ were computed coincident with a vertical dipole transmitter at 81 placements on a 9 x 9 grid with 0.4 m spacing. An observation time of 610 μs after transmitter turn-off was chosen to approximate the effective center time of the averaging gate of a commerical transmitter-receiver system (Geonics EM-61). The largest observed derivative component is $dB_z^{(s)}/dt$ directly above the sphere. For a 180 Amp-

m^2

transmitter moment, $dB_z^{(s)}/dt$ = -4648. nT/s for the measurement directly above the sphere at 610 μs. Gaussian noise of magnitude 8.8 nT/s was added to the $dB_z^{(s)}/dt$ measurements simulating an observed noise level (at Fort Ord, California). Gaussian noise of magnitude 27. nT/s was added to the $dB_x^{(s)}/dt$ and $dB_y^{(s)}/dt$ measurements to simulate the larger noise levels typically observed in horizontal field components.

This data was inverted for dipole polarizabilities and location. The downhill simplex algorithm converges to a weighted rms misfit of 0.90318 with the estimated object center at (x,y,z) = (0.0028, -0.0039, 1.0008) meters. Started from this point, after two iterations the linearized inversion converges to a weight rms misfit of 0.90316 with the estimated object center at (0.0026 ±0.0030, -0.0040 ±0.0030, 1.0002 ±0.0051) meters. The true center position is (0,0,1) meters. The estimated principal dipole polarizabilities L_{11}, L_{22}, and L_{33} are -0.655 ±0.015, -0.647 ±0.011, -0.635 ±0.014 Amp-m^2/s/μT. The absolute differences between principal dipole polarizability estimates 0.008 ±0.010 and 0.012 ±0.009 Amp-m^2/s/μT respectively for $|L_{11}-L_{22}|$ and $|L_{22}-L_{33}|$, are less than two estimation errors, indicating that the object is spherically symmetric within measurement errors. One also could surmise the object's sphericity directly from the raw polarizability matrix estimates before rotation to estimated principal coordinates: $(m_{xx}, m_{yy}, m_{zz}, m_{xy}, m_{yz}, m_{xz})$ = (-0.6490 ±0.0087, -0.6418 ±0.0085, -0.6461 ±0.0199, 0.0006 ±0.0027, 0.0081 ±0.0059, -0.0039 ±0.0058) Amp-m^2/s/μT; the off-diagonals are smaller than twice their uncertainties, and the diagonal elements agree to within their uncertainties.

As previously noted, when comparing uncertainties for instrument design purposes, one can eliminate the small dependence of uncertainty estimates on the particular realisation of noise added to simulated data, by evaluating the coefficient matrix using the true object position and polarizability matrix. Doing this yields the expected values for the equivalent dipole position uncertainties, 0.0031, 0.0031, and 0.0053 meters, and the expected values for the unrotated moment uncertainties, (±0.0093,

±0.0093, ±0.0204, ±0.0028, ±0.0062, ±0.0062) $Amp^2/s/\mu T$, slightly different than the previous uncertainty estimates.

With synthetic data, error estimates may also be obtained by Monte Carlo simulation, by rerunning a simulation repeatedly with different realizations of the simulated noise, and computing standard deviations of the resulting estimates. Rerunning the inversion of data from a simulated 12 cm diameter steel sphere 1000 times, with different Gaussian noise realizations, the standard deviations of the 1000 estimates of object center location coordinates are 0.0029, 0.0030, and 0.0050 meters. Monte Carlo standard deviations for the unrotated polarizability matrix elements **m** are (±0.0086, ±0.0086, ±0.0196, ±0.0026, ±0.0059, ±0.0056) $Amp^2/s/\mu T$. Monte Carlo standard deviations for the principle polarizabilities are 0.014, 0.010, and 0.014 $Amp\text{-}m^2/s/\mu T$. Given that the relative error in the Monte Carlo uncertainty estimates is 4.5%, the Monte Carlo values compare well with the expected values for the uncertainties.

For similar synthetic data from a 8 cm diameter buried steel sphere in the same position with the same added noise, the algorithm converges to a weighted rms misfit of 0.90292 with the estimated object center at (0.0114 ±0.0127, -0.0173 ±0.0130, 1.0078 ±0.0217), and principal polarizabilities -0.169 ±0.018, -0.159 ±0.011, -0.148 ±0.012 $Amp\text{-}m^2/s/\mu T$, with absolute differences of 0.010 ±0.010 and 0.011 ±0.008 $Amp\text{-}m^2/s/\mu T$ respectively. At 610 μs, the 8 cm sphere has a polarizability 0.24 times smaller than the 12 cm sphere. The uncertainties in position are approximately four times larger for the smaller sphere consistant with its decreased polarizability. The principal polarizability uncertainties differ from those for the 12 cm sphere as the estimated principal directions are different in the two cases, the estimated principal directions being controlled by the noise, in the absence of any underlying anisotropy of the target. The uncertainties in the elements of the unrotated polarizability matrices agree more closely: **m** = (-0.161 ±0.009, -0.154 ±0.008, -0.161 ±0.021, 0.001 ±0.003, 0.009 ±0.006, -0.004 ±0.006) $Amp^2/s/\mu T$. The differences between the uncertainties here and those for unrotated polarizability matrix estimates for the 12 cm diameter sphere are on the order of the differences between each and their expected values.

For a second example, the response of an aluminum prolate spheroid 24 cm long by 8 cm wide, of conductivity $\sigma = 3.5\ 10^7\ \Omega^{-1} m^{-1}$ was modelled using an integral equation code provided by P. B. Weichman of Blackhawk Geophysics, with subsequent modifications to improve accuracy. The code expands the electric field within the spheroid in a polynomial basis, and solves for a set of modes, each with a characteristic decay time. Subsequently, the excitation of the modes for each position of transmitter loop is computed for a ramp-on/ramp-off transmitter current, and the contributions of the different mode voltages observed in receiver coils are summed over modes, for each transmitter-receiver pair. This code was used to compute the spheroid response for 81 transmitter loop positions of a 1m square horizontal loop, on a 9 by 9 grid with 0.2m spacing, in two coaxial dipole receivers, one concentric with the transmitter, and the other 0.4m above the first. The spheroid center was placed 0.6m below the transmitter level, offset 0.2m in x and y from the grid center, with symmetry axis in the $y-z$ plane dipping -30°. A 3.3 ms ramp-on, 0.08 ms ramp-off transmitter current, and a 0.4 ms averaging gate starting 0.42 ms after transmitter current extinction, were used to emulate a commercial transmitter-receiver system (Geonics EM-61).

Gaussian noise with a magnitude of 1% of the largest observed voltage was added to the computed voltages. The resultant data was inverted, yielding an estimated center location of (0.207 ±0.008, 0.206 ±0.009, 0.600 ±0.005) meters, in agreement with the true location (0.200, 0.200, 0.600). The principal polarizabilities were estimated as 0.785 ±0.023, 0.768 ±0.018, and 0.529 ±0.011 V/μT, with differences 0.016 ±0.025 and 0.238 ±0.020 V/μT. The agreement of L_{11} and L_{22} indicates an object that, within measurement errors, is rotationally symmetric about the third principal direction. The differences between the third moment and the other two are well resolved, and, for a non-magnetic object, consistent with the smaller cross section perpendicular to the symmetry axis. The third principal direction is estimated as (0.016 ±0.023, 0.850 ±0.026, -0.526 ±0.043), in agreement with the true axis of symmetry (0, 0.866, -0.500).

In these examples, the downhill simplex method works well to find the global minimum of the data misfit as the data misfit has a large "valley" in data misfit sloping downwards to a well defined minimum at the object center (within measurement errors). An example of data misfit for an instrument configuration which results in a secondary minimum in data misfit near the global minimum, is shown in Figure (1), for the system of the first example, without its two horizontal component receivers. There is a clear minimum by the true object center at (0,0,1) m, but also a local minimum at (-0.02, 0.00, 1.11) meters. For analyzing data from such as system, a more general optimization method must be substituted for the downhill simplex method used in this paper. Restoring the horizontal field receivers, eliminates the secondary minimum, as shown in Figure (2). With current day computing, it may be advantageous to use transmitter-receiver systems which allow the use of the downhill simplex method used here, to allow real time fitting of equivalent dipole polarizabilities and locations.

ACKNOWLEDGEMENTS

This work was supported by the US Department of the Army under Contract No. W74RDV93447299.

REFERENCES

C. E. Baum, ‘‘Low frequency near-field magnetic scattering from highly conducting, but not perfectly conducting bodies,’’ in C. E. Baum, Ed., *Detection and Identification of Visually Obscured Targets*, Philadelphia: Taylor et Francis, ch. 6, pp. 163-217, 1999.

T. H. Bell, B. J. Barrow, and J. T. Miller, ‘‘Subsurface discrimination using electromagnetic induction sensors,’’ *IEEE Trans. Geosci. Remote Sensing*, vol. 39, no. 6, pp.1286-1293. June 2001.

J. D. Jackson, *Classical Electrodynamics, Second Edition.* New York: John Wiley and Sons, 1975.

N. Khadr, B. J. Barrow, T. H. Bell, and H. H. Nelson, ‘‘Target shape classification using electromagnetic induction sensor data,’’ in *Proceeding of UXO Forum* 1998.

L. R. Pasion and D. W. Oldenburg, ‘‘Locating and determining dimensionality of UXOs using time domain elecromagnetic fields,’’ *Journal of Environmental and Engineering Geophysics*, vol. 6, no. 2, pp. 91-102, June 2001.

W. H. Press, B. P. Flannery, S. A. Teukolsky, and W. T. Vetterling, *Numerical Recipes, the Art of Scientific Computing.* Cambridge: Cambridge University Press, 1986.

L. D. Landau and E. M. Lifshitz, *Electrodynamics of Continuous Media.* Reading: Addison-Wesley, 1960.

G. S. Watson, *Statistics on Spheres.* New York: Wiley-Interscience, 1983.

Figure Captions

Figure (1). Squared data misfit as a function of candidate object center position $\mathbf{r}_o$, for vertical dipole transmitter, coincident vertical dipole receiver system sited on a 9x9 grid with 0.4m spacings, centered 1 m above a 12 cm diameter steel sphere at (0,0,1) m.

Figure (2). Squared data misfit as a function of candidate object center position $\mathbf{r}_o$, for vertical dipole transmitter, coincident 3 component receiver system sited on a 9x9 grid, centered 1 m above a 12 cm diameter steel sphere at (0,0,1) m.

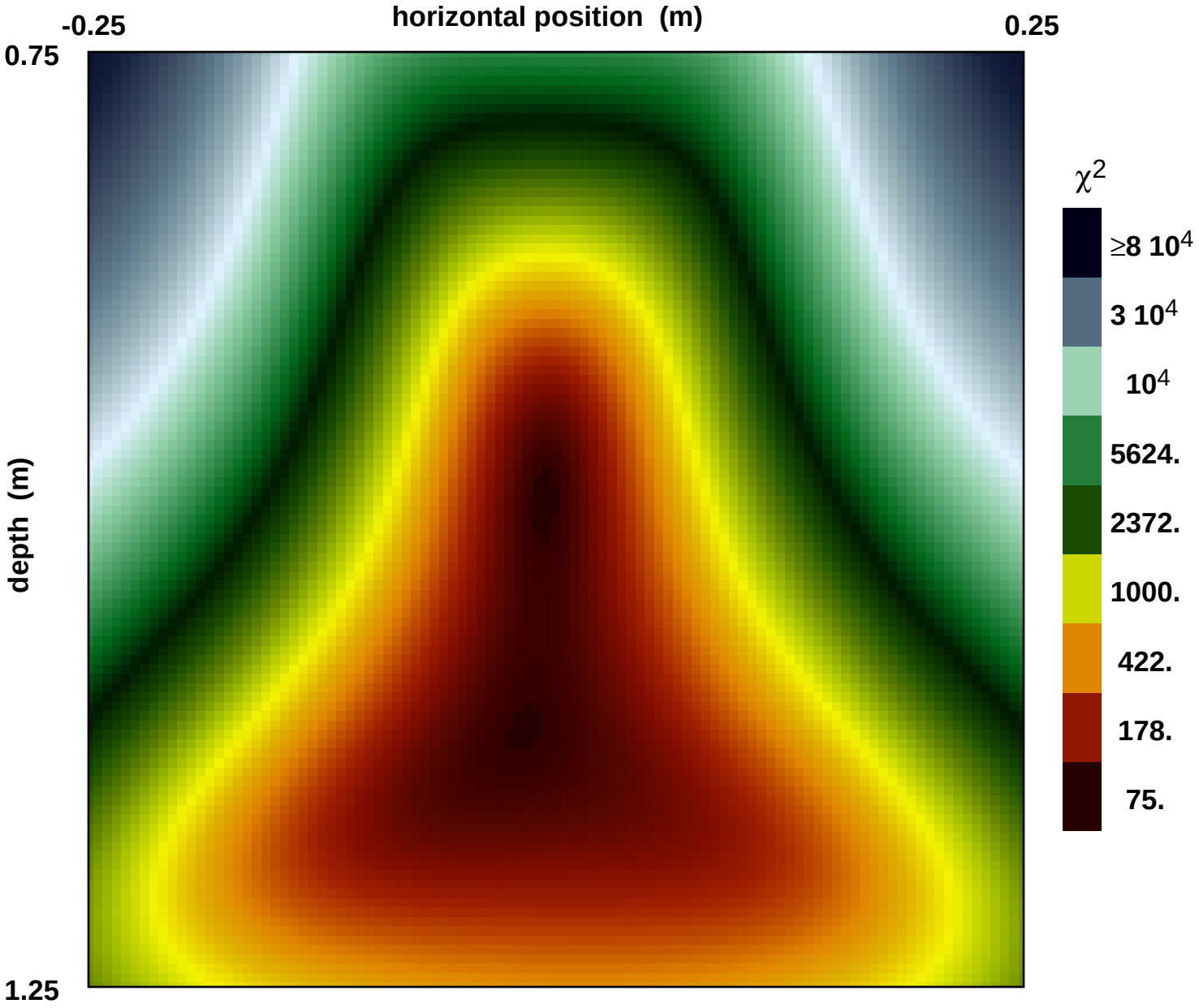
horizontal position (m)
-0.25
0.25
0.75
1.25
depth (m)
χ^2
≥8 10^4
3 10^4
10^4
5624.
2372.
1000.
422.
178.
75.

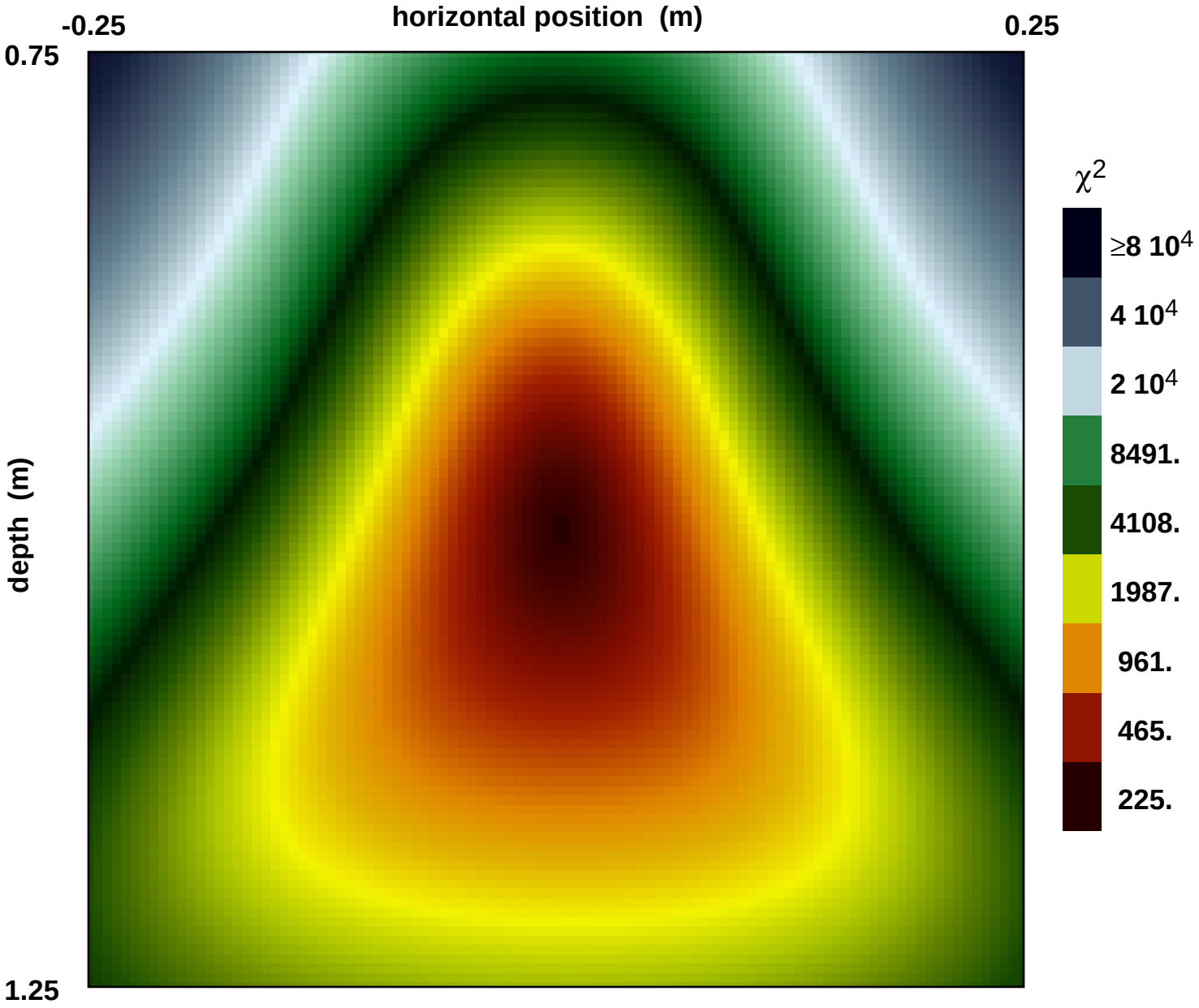
horizontal position (m)
-0.25
0.25
0.75
1.25
depth (m)
χ^2
≥8 10^4
4 10^4
2 10^4
8491.
4108.
1987.
961.
465.
225.